

Discrete bright solitary waves in quadratically nonlinear media

T. Peschel,^{*} U. Peschel, and F. Lederer[†]

Institut für Festkörperteorie und Theoretische Optik, Friedrich-Schiller-Universität Jena, Max-Wien-Platz 1, D-07743 Jena, Germany

(Received 13 May 1997)

We show that bright solitary waves of different topologies can exist in a discrete system with a quadratic nonlinearity. Analytical solutions can be derived for a limiting case. The regions of existence and stability are identified. We numerically study interaction and collision phenomena. Various decay scenarios for unstable solutions are discussed. [S1063-651X(98)00801-0]

PACS number(s): 42.65.Tg, 42.65.Ky

I. INTRODUCTION

Within the past several years the interest in nonlinear optical effects based on quadratic nonlinearities has considerably renewed. In contrast to previous studies where the attention was primarily centered on the dynamics of the frequency conversion process (second-harmonic generation, parametric effects) recent work focuses on the phase modulation of the fundamental (FH) as well as the second harmonic (SH). This phase modulation accompanies the familiar amplitude modulation, being the basis of any frequency conversion, and may be obviously exploited in fields that have been considered the arena of cubic nonlinear effects. Typical examples are all-optical switching phenomena in interferometric or coupler configurations as well as spatial and temporal solitary wave formation in planar waveguides (for a review, see Ref. [1] and the references therein). Frequently it was attempted to explain these effects in terms of an effective cubic nonlinearity. But it turned out that the quadratic scenario may be potentially richer evidenced by recent results such as, e.g., an incoherent switching scheme [2], the formation of stable solitary waves in bulk media [3], the homogeneous phase modulation across a short pulse [4], the existence of stable chirped solitary waves [5,6], and the peculiar features of Bragg grating solitary waves [7].

Another fundamental issue that has attracted much attention in various configurations with cubic nonlinearities and that to our knowledge has not been addressed in the quadratic environment until now, is the existence and stability of intrinsic localized solutions in discrete systems. In the cubic case the study of these solutions, often referred to as discrete self-trapped solutions or discrete solitary waves, is a major subject in nonlinear physics since the pioneering work of Fermi, Pasta, and Ulam [8]. The relevant topic of these studies is how discreteness affects the dynamics of nonlinear systems beyond the continuum approximation. Recently, it was pointed out (see, e.g., Refs. [9,10] and the references therein) that arrays of nonlinear waveguides may represent a convenient laboratory to experimentally verify the numerous theoretical predictions. Thus it seems worthwhile to study the effects of discreteness in quadratic nonlinearities in that

environment. Field dynamics in a linearly coupled array of nonlinear waveguides may be considered as a general case that covers two limiting cases, viz., spatial solitary wave formation in a planar waveguide (continuous limit) and nonlinear switching in a two-core coupler. For quadratic nonlinearities both effects have been theoretically predicted [11,12] and experimentally confirmed recently [13,14]. Hence it can be anticipated that such intrinsic localized solutions, henceforth termed discrete solitary waves (DSWs), may be formed in quadratic nonlinear waveguide arrays as well. The peculiarities of DSWs in cubic materials with respect to their continuous counterparts, such as the existence of bright spatial DSWs in defocusing media, are mainly due to the particular dispersion relation of the linear waves, which allows for “negative diffraction” if the envelopes in adjacent waveguides have opposite phases (staggered solutions [15]). So it is intuitively clear that similar solutions should also arise in the quadratic case but it can be also expected that the existence of a two-component field (FH and SH) with different linear properties of each component will add more degrees of freedom to the solution. Because of the waveguide dispersion and the frequency dependence of linear coupling FH and SH propagate as a matter of fact in different arrays. Moreover, the wave vector mismatch between the FH and the SH will strongly affect the character of nonlinear interaction, i.e., its sign controls the sign of phase modulation [4]. Eventually it is anticipated that localization, which is a typical effect of discreteness [16], depends on the explicit form of the nonlinearity.

The aim of this paper is to identify regions of existence for discrete solitary waves in arrays of quadratically nonlinear waveguides, to discuss their basic properties, and to investigate their mutual interactions. Particular emphasis is paid to effects that are peculiar for quadratic nonlinearities. The structure of the paper is as follows: In Sec. II we derive the basic equations as well as the nonlinear dispersion relation. Stationary discrete solitary wave solutions are analytically and numerically derived in Sec. III. The investigation of the dynamical behavior of these solutions (stability, interactions, collisions) in Sec. IV concludes the paper.

II. THE NONLINEAR DISPERSION RELATION

In the framework of a coupled-mode theory the continuous wave evolution of the envelopes of the FH (u_n) and the SH modes (v_n) in the n th guide can be described by a sys-

^{*}Present address: Fraunhofer-Institut für Angewandte Optik und Feinmechanik, Schillerstr. 1, 07745 Jena, Germany.

[†]Electronic address: p6peul@uni-jena.de

tem of ordinary differential equations. In deriving that system one can take advantage of recent works concerning arrays formed by cubic nonlinear waveguides [9] and continuous systems (e.g., planar waveguides) with quadratic nonlinearities [4,17]. We straightforwardly get

$$\text{FH: } i \frac{du_n}{dz} + c_u(u_{n+1} + u_{n-1}) + 2u_n^* v_n = 0, \quad (1a)$$

$$\text{SH: } i \frac{dv_n}{dz} + c_v(v_{n+1} + v_{n-1}) - \Delta v_n + u_n^2 = 0. \quad (1b)$$

Here we have assumed that the guides are identical, that only nearest neighbor interaction, expressed by the linear coupling constants $c_{u,v}$, takes place, and that the nonlinear coupling is relevant only between FH and SH in the same guide. Equation (1) is normalized as usual where the length and the power scales are set by one of the inverse linear coupling constants and the quadratic nonlinear coefficient, respectively [4,9], and Δ denotes the scaled wave vector mismatch between FH and SH. It is evident that either c_u or c_v amount then to unity but we maintain the general notation for the sake of flexibility. In relevant waveguide arrays arbitrary ratios c_u/c_v can be achieved. One might anticipate that the confinement of the SH mode is stronger than that of the FH, implying $c_u/c_v > 1$. But if the dispersion of the host exceeds that of the core material the opposite situation with strongly coupled SH modes occurs.

The system (1) has two conserved quantities that can be used to characterize DSW solutions, i.e., the guided power

$$E = \sum_{n=-\infty}^{\infty} (|u_n|^2 + 2|v_n|^2) \quad (2a)$$

and the Hamiltonian

$$H = - \sum_{n=-\infty}^{\infty} (c_u u_n^* u_{n+1} + c_v v_n^* v_{n+1} + u_n^2 v_n^* - \frac{1}{2} \Delta |v_n|^2 + \text{c.c.}). \quad (2b)$$

In order to identify the region where DSWs may exist it is convenient to inspect the dispersion relation of a plane wave solution

$$u_n(z) = u_0 \exp[i(\lambda_{\text{pw}} z + \kappa n)]$$

and

$$v_n(z) = v_0 \exp[2i(\lambda_{\text{pw}} z + \kappa n)],$$

which relates the propagation constant λ_{pw} to the transverse wavenumber κ . This relation depends on the power carried by the FH and reads as

$$[\lambda_{\text{pw}} - c_v \cos(2\kappa) + \Delta/2] [\lambda_{\text{pw}} - 2c_u \cos(\kappa)] - |u_0|^2 = 0. \quad (3)$$

Obviously, the existence of bright DSWs requires two prerequisites, viz., their wave vectors λ have to be situated in regions in the κ - λ plane where (i) linear plane waves [real-valued solutions of Eq. (3) for $|u_0|^2 = 0$] must not exist, but

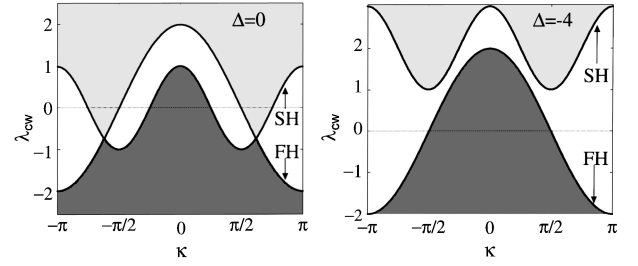


FIG. 1. Nonlinear continuous waves in the plane defined by the propagation constants λ_{cw} and the transverse wavenumber κ for different values of the phase mismatch Δ ; $c_u=1$, $c_v=1$; dark gray area: antiphase waves, light gray area: in-phase waves, white area: no waves, bold lines: linear dispersion relation of FH and SH.

(ii) nonlinear plane waves are allowed to propagate. In Fig. 1 the linear dispersion relation of both waves is marked by solid lines. In the shaded areas nonlinear plane waves are permitted. Thus the DSW wave number λ has to be located outside the bands defined by the respective linear dispersion relations. Note that the mismatch Δ plays a significant role in determining the corresponding region. So, we can conclude that bright DSWs may exist either for

$$\lambda > \max(2c_u, c_v - \Delta/2) \quad (4a)$$

or for

$$\lambda < \min(-2c_u, -c_v - \Delta/2). \quad (4b)$$

This splitting in the wave vector domain is a typical effect of discreteness. In continuous systems where the linear dispersion is essentially parabolic the relevant wave-vector region is connected and the wave vectors are either positive or negative. In arrays with a cubic nonlinearity a transition from one region to the other can be achieved by simultaneously changing the sign of nonlinearity and the phase between adjacent guides by π (transition from staggered to unstaggered solutions or vice versa). This is due to the invariance of the relevant dynamic equation with respect to these transformations. In the quadratic scenario the situation is more involved because this invariance does not hold.

III. DISCRETE SOLITARY WAVE SOLUTIONS

After having identified the regions where DSWs may exist we are going to derive the explicit solutions in this section. In looking for stationary DSW solutions to Eq. (1) we introduce the ansatz $u_n(z) = u_n \exp(i\lambda z)$ and $v_n(z) = v_n \exp(2i\lambda z)$ into Eq. (1) and exploit that these solutions are real valued (except of a trivial phase transformation $u_n \rightarrow u_n e^{i\varphi}$, and $v_n \rightarrow v_n e^{2i\varphi}$) to get

$$-\lambda u_n + c_n(u_{n+1} + u_{n-1}) + 2u_n v_n = 0, \quad (5a)$$

$$-2\lambda v_n + c_v(v_{n+1} + v_{n-1}) - \Delta v_n + u_n^2 = 0. \quad (5b)$$

As a matter of fact the system (5) can only be solved numerically and we are going to do that later. But to get some insight into the general tendencies we investigate two limiting cases first. If the coupling for one of the two frequency components disappears, the system simplifies considerably,

and basic features of the solutions that are determined by the remaining energy transfer process are illuminated in more detail. Strictly speaking zero coupling is never achievable. However, the coupling strength can vary considerably. It decreases exponentially with the square root of the difference between the effective index of the guided mode and that of the cladding material. If the dispersion of the cladding differs strongly from that of the core either coupling constant will always be very small.

We study the limiting case of vanishing coupling of the SH components first ($c_u=1, c_v=0$). Then the system simplifies to a familiar case. From Eq. (5b) we get $v_n = u_n^2 / (2\lambda + \Delta)$ and subsequently the system (5) is reduced to

$$\lambda u_n = u_{n+1} + u_{n-1} + \frac{2}{2\lambda + \Delta} |u_n|^2 u_n, \quad (6)$$

which constitutes the cubic or Kerr limit (see, e.g., Refs. [9, 15, 18, 19]). Depending on the magnitude and sign of wave number λ and detuning Δ the effective cubic nonlinearity may be either focusing or defocusing. A peculiarity of this limit is that in the same array (fixed quadratic nonlinearity, fixed coupling constants) bright unstaggered ($2\lambda + \Delta > 0$) as well as staggered ($2\lambda + \Delta < 0$) DSWs can coexist, which contrasts the conventional cubic case. Within this Kerr limit both kinds of DSWs exhibit a similar intensity profile. As we are going to show below this symmetry is destroyed if the SH components are allowed to couple (see Fig. 2). For the cubic scenario it has been shown that approximate analytic solutions can be found for highly localized states (only 3 or 4 guides are participating in the coupling process) [18]. That technique could be likewise exploited here. Because the cubic (Kerr) case was intensively studied in the literature (see,

e.g., [9] and the references therein) we leave this limit and consider the opposite situation where merely the SH waves couple ($c_u=0, c_v=1$). Because the complete energy exchange is mediated by the SH wave we can expect to identify peculiar effects introduced by the quadratic nonlinearity. In addition a one parameter family of stationary SWs can be determined analytically in this limiting case. Now Eq. (5a) supports two types of solutions for arbitrary n , viz., either a vanishing FH ($u_n=0$) or an arbitrary fundamental but fixed SH ($v_n=\lambda/2$). In both cases the complementary field (SH or FH) can be calculated by using Eq. (5b). It is easy to verify that in the first case the SH exhibits an exponential decay provided that Eq. (4) holds. Now in combining both types of solutions various DSWs can be formed. Here we restrict ourselves to the simplest ones, which exhibit characteristic peculiarities of DSWs in quadratic media, namely, unstaggered and staggered DSWs that may be centered either on a single waveguide (field is located at an *odd* number of guides—odd DSWs) or between two adjacent waveguides (field is located at an *even* number of guides—even DSWs).

To get more specific the odd and even analytical solutions of Eq. (5) can be now written as

$$u_n^{(\text{odd})} = \delta_{n,0} \sqrt{\lambda(\lambda - \alpha + \Delta/2)}, \quad v_n^{(\text{odd})} = \frac{\lambda}{2} \alpha^{|n|}, \quad (7a)$$

$$u_n^{(\text{even})} = (\delta_{n,0} + \delta_{n,1}) \sqrt{\lambda[\lambda - (\alpha - \Delta + 1)/2]},$$

$$v_n^{(\text{even})} = \frac{\lambda}{2} \alpha^{|n-1/2|-1/2}, \quad (7b)$$

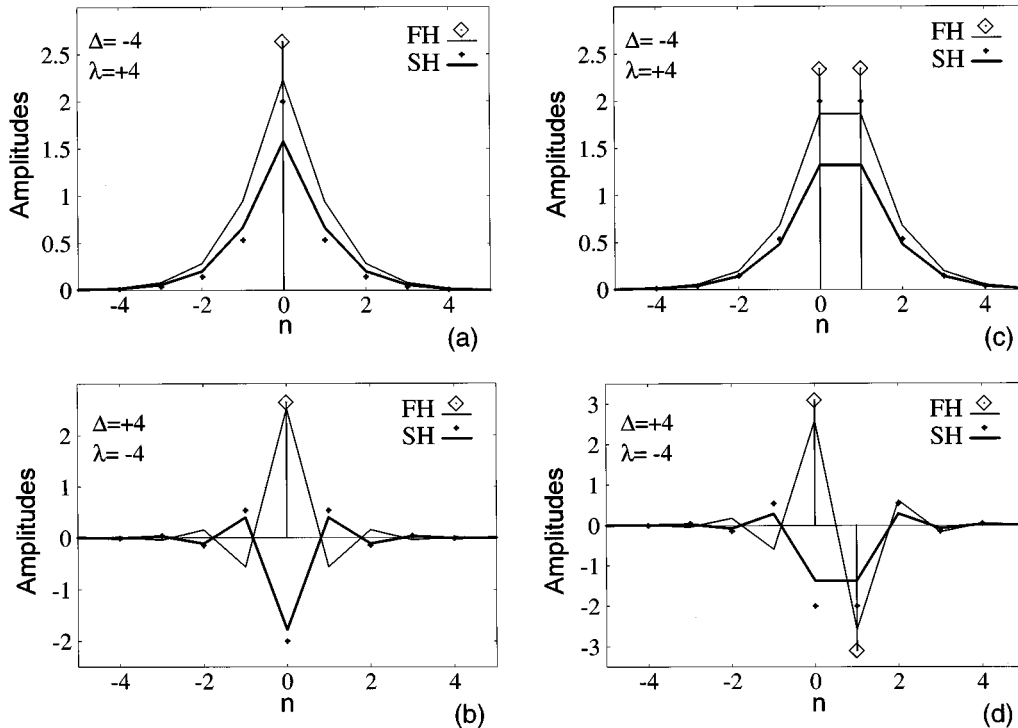


FIG. 2. Field profiles of the basic bright DSWs. Symbols: analytical model ($c_u=0$ and $c_v=1$); lines: general case with equal coupling strength for FH and SH ($c_u=1$ and $c_v=1$). (a) Odd, unstaggered; (b) odd, staggered; (c) even, unstaggered; (d) even, staggered.

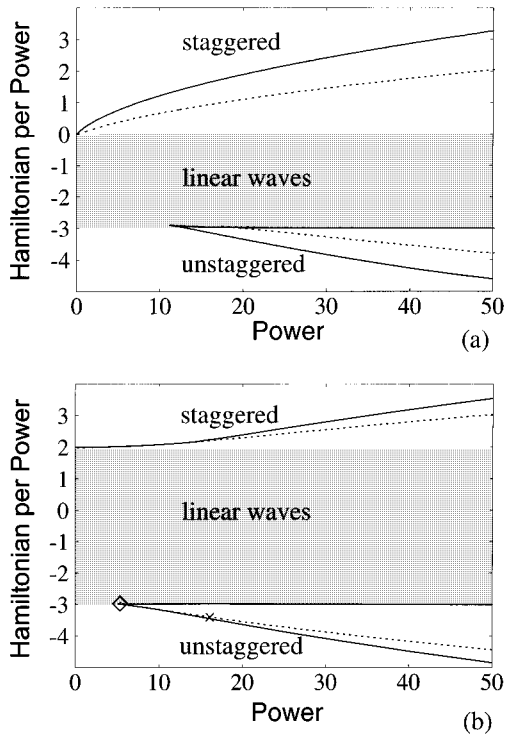


FIG. 3. Normalized Hamiltonian vs power for DSWs of different topology ($\Delta = -4$). (a) Analytical model ($c_u = 0$ and $c_v = 1$), (b) general case ($c_u = 1, c_v = 1$). Solid lines: odd DSWs; dashed lines: even DSWs.

respectively, where the sign of the FH fields is arbitrary. Here

$$\alpha = \left(\alpha + \frac{\Delta}{2} \right) \left[1 - \left(1 - \frac{4}{(2\lambda + \Delta)^2} \right)^{1/2} \right] \quad (7c)$$

characterizes the decrease of the SH amplitude with distance from the center where $\alpha > 0$ and $\alpha < 0$ hold for the unstaggered and staggered DSWs, respectively. From the condition that both α and u_n have to be real valued and $|\alpha| < 1$ has to hold we obtain the regions of existence of DSWs as $\lambda > \max(0, 1 - \Delta/2)$ for unstaggered and $\lambda < \min(0, -1 - \Delta/2)$ for staggered DSWs, which is consistent with Eq. (4). Note that the condition for the existence of staggered DSWs ($2\lambda + \Delta < 0$) is identical to that in the Kerr limit.

Now we drop the condition of a vanishing coupling constant of the FH and solve Eq. (5) numerically for the more general case of equal coupling of the FH and the SH, i.e., $c_u = c_v = 1$. The results are also useful for double checking the performance of our analytical model. In Fig. 2 the profiles of the four basic types of DSWs introduced above are sketched as obtained by both models. It is evident that the characteristic features of DSWs are maintained in the analytical model. However, it is clear that in this limiting case the FH is only excited in a single (odd DSW) or in two (even DSW) adjacent guides, respectively.

IV. DYNAMICAL EFFECTS—STABILITY, INTERACTIONS, COLLISIONS

After having identified the simplest stationary DSWs we are going to study their dynamical behavior, where primary concern is paid to their stability. But it is also interesting to look to the collision behavior, which should exhibit the features typically encountered in nonintegrable systems. It is clear that the latter issue has to be addressed in using numerical means. But with regard to the stability and localization behavior we can exploit a standard procedure frequently used in discrete systems. It has been suggested [19] that even and odd DSWs of the same topology and with the same guided power can be considered as realizations of a common mode but centered at or in-between the array elements. Then the difference in the respective Hamiltonians represent likewise the so-called Peierls-Nabarro barrier (PNB) [15,19]. The realization where the Hamiltonian attains an extremum is considered stable. Moreover, the PNB is a measure for the localization of the DSW, i.e., if the barrier is sufficiently small the solution can move across the array consecutively changing from one realization to the other. We carry out our analysis for the analytical model ($c_u = 0$) as well as the general case ($c_{u,v} \neq 0$) where we make use of the numerical solutions in the latter case and compare the respective results. In the analytical model the guided power (2a) and the Hamiltonian (2b) can be straightforwardly calculated by using Eq. (7) as

$$E^{(\text{odd})} = \frac{\lambda^2}{2} \frac{1 + \alpha^2}{1 - \alpha^2} + \lambda \left(\lambda - \alpha + \frac{\Delta}{2} \right), \quad (8a)$$

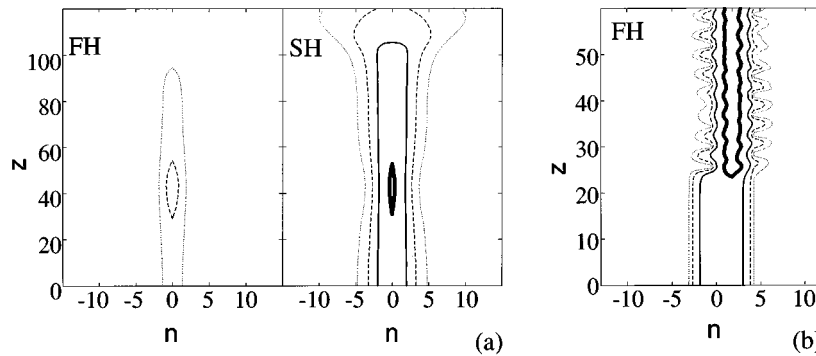


FIG. 4. Evolution of unstable unstaggered DSWs ($\Delta = -4$). (a) Decay of an unstable odd SW ($\lambda = 3.05$) labeled by a diamond in Fig. 3(b). (b) Transformation of an unstable even DSW into an odd DSW ($\lambda = 4$) labeled by a cross in Fig. 3(b); contour lines at 4, 2, 1, 0.5.

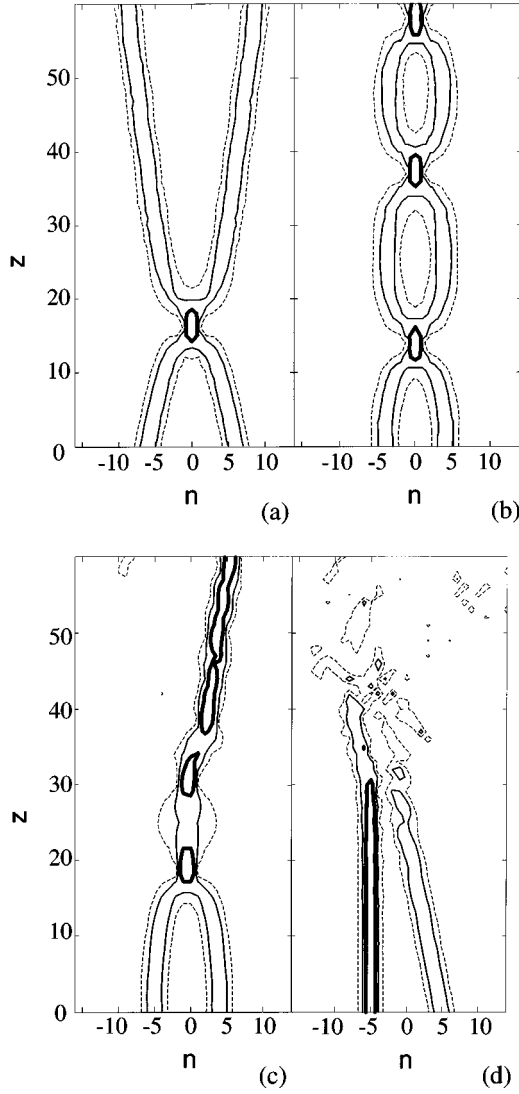


FIG. 5. Power-dependent steering of a beam across the array ($\Delta=0$, $c_u=1$, $c_v=1$). Initial shape: that of an unstaggered DSW ($\lambda=2.5$), but with an initial phase tilt of 0.1 per channel and with different power levels.

$$\begin{aligned}
 H^{(\text{odd})} &= -\lambda^2 \frac{\alpha - \frac{\Delta}{4}(1 + \alpha^2)}{1 - \alpha^2} - \lambda^2 \left(\lambda - \alpha + \frac{\Delta}{2} \right), \\
 E^{(\text{even})} &= \frac{\lambda^2}{1 - \alpha^2} + 2\lambda \left(\lambda - \frac{\alpha - \Delta + 1}{2} \right), \\
 H^{(\text{even})} &= -\lambda^2 \frac{\alpha - \frac{\Delta}{2}}{1 - \alpha^2} - \frac{\lambda^2}{2} - 2\lambda^2 \left(\lambda - \frac{\alpha - \Delta + 1}{2} \right) \quad (8b)
 \end{aligned}$$

for odd and even DSWs, respectively.

To discuss the stability behavior it is convenient to plot the Hamiltonian normalized by the guided power versus the guided power. The plots for both cases are shown in Fig. 3 where the qualitative agreement is evident. A straightforward estimation, by using Eq. (2), yields that the absolute value of

the normalized Hamiltonian for DSW exhibits an upper bound as $[|H/E| < (2c_u + c_v + |\Delta/2 + \sqrt{2E}|)]$ whereas for linear waves this absolute value lies in a band around zero, i.e., $\min(-2c_u, \Delta/2 - c_v) < H_{\text{lin}}/E < \max(2c_u, \Delta/2 + c_v)$. We expect the value of the Hamiltonian applying to DSWs to be located outside that band but between the upper and the lower bound. In the limit of extreme localization ($\lambda \rightarrow \pm\infty$) both E and H tend to infinity. In the opposite case where the wave number λ approaches the linear spectrum [see Eq. (4)] two different cases have to be distinguished (see also Fig. 1). If the boundary is set by the linear spectrum of the FH (for staggered and/or unstaggered DSWs: $2c_u > c_v \pm \Delta/2$) both the power and the Hamiltonian vanish simultaneously. This corresponds to the upper branches in Figs. 3(a) and 3(b), e.g., $\lambda=0$ in the analytical model. On the contrary if the boundary is set by the SH (for staggered and/or unstaggered DSWs: $2c_u < c_v \pm \Delta/2$) both quantities diverge due to a spreading SH field ($\alpha=1$ in the analytical model). This result can be easily verified in the analytical model where the denominator vanishes in Eq. (7c). As a consequence a power threshold for the DSWs together with a backbend branch in the Hamiltonian versus energy plot exists [see lower area in Figs. 3(a) and 3(b), e.g., $\lambda = \pm 1 - \Delta/2$ in the analytical model]. We note that this threshold can appear for either topology of DSWs depending on where E and H diverge. At the turning point the odd as well as the even solutions transform to solutions of similar shape but different distribution between the FH and SH components. These backbend branches coincide for even and odd modes for our set of parameters. The results with respect to the stability of DSWs can be summarized by using Fig. 3 as follows.

Both models yield that odd staggered as well as unstaggered DSWs may be stable whereas their even counterparts are always unstable. They immediately transform into the respective odd DSWs. If odd DSWs of one topology have a finite power threshold the backbend branch near the linear band is unstable. This instability manifests itself in a complete decay of the DSW into linear waves. It is interesting to note that this instability beyond the turning point is accompanied by a power transfer to the SH and a complete spreading of that power across the array [see Fig. 4(a)].

In some respects it is surprising that our analytical model predicts the stability behavior correctly. We note that the existence of a power threshold is a peculiarity of the quadratic system. The stability predictions based on the study of the Hamiltonian and the related PNB could be confirmed in performing a conventional linear stability analysis.

Moreover these results have been double checked by numerically solving Eq. (1) with the DSW to be probed as the initial distribution. To perturb the stationary solution even harder we have added some stochastic noise to this initial distribution. In Fig. 4(a) the decay of an unstable odd unstaggered DSW that belongs to a backbend branch [diamond in Fig. 3(b)] is shown. As mentioned above the power is transferred to the SH, which spreads over the array. Note that in the continuous case this unstable solitary wave with an excess power would not decay completely but transform into a solitary wave oscillating around a stable solution [20].

Next we excited an unstable even unstaggered DSW [cross in Fig. 3(b)]. After some propagation distance it transforms to a slightly oscillating, but stable odd DSW [see Fig.

4(b)]. In some respect this transformation can be regarded as the onset of localization, which is a peculiarity of discrete systems. Relying on the idea of a Peierls-Nabarro barrier introduced above it is clear from Fig. 3 that the solutions obtained for the limiting case of vanishing coupling between the FH waves are always localized. Thus the unstable even solutions transform into a resting, but oscillating, stable odd realization. In this case we did not succeed in exciting moving solutions. Energy transfer and motion across the array seem to be mediated by the FH wave. Indeed, staggered as well as unstaggered DSWs exhibit an almost vanishing PNB for small power if the coupling in the FH is taken into account [see Fig. 3(b)]. This leads to the conclusion that up to a certain power level DSWs of both topologies can move across the array. This power dependent dynamical behavior of discrete DSWs can be exploited in a beam steering experiment (see Fig. 5). Assuming a nonlocalized DSW an initial phase tilt causes the solution to move across the array without changing its shape. If the power is increased the same scenario as discussed above in the analytical model can be observed. The PNB between the unstable even DSW and the odd one grows larger and localization sets in. Eventually all the power rests in the initial wave guide which decouples from the rest of the array. Hence a continuous power increase allows one to address different waveguides at the end facet of the device.

Finally we performed numerical experiments to study collisions and interactions of two moving DSWs. From what was said above it is clear that these studies can be only performed if the solutions are not localized. Thus we have to take the coupling of the FH into account and to rely on the numerical solutions. Again we used a stable odd DSWs but imposed a slight phase difference between adjacent guides to provoke the motion across the array if required as in Figs. 6(a) and 6(b). Due to the inherent complexity of the system many different scenarios may occur. First we collided two moving unstaggered solutions. Figure 6(a) shows a typical scenario if the velocity is large, e.g., a mere phase shift due to the collision. By decreasing the velocity below a certain critical value the DSWs fuse, which is an indication for the nonintegrability of the system (1). This behavior is in agreement with that in the quadratic continuous case [21]. If the separation between both DSWs decreases and the initial velocity is set to zero we have observed an interaction behavior recalling the formation of a certain kind of bound state. That very scenario appears if the DSWs collide on-site [see Fig. 6(b)].

If a slight change in the initial separation causes a collision between two waveguides the interaction leads to the formation of an intermediate unstable even DSW. Finally it translates into a moving DSW [Fig. 6(c)].

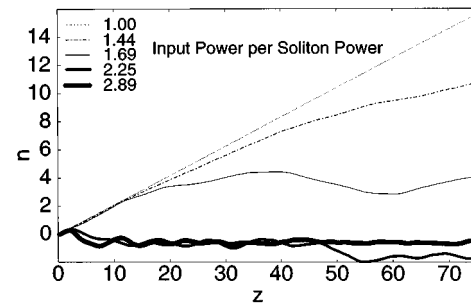


FIG. 6. Collisions and interactions of DSWs ($\Delta=0$, $c_u=1$, $c_v=1$). (a) Elastic collision of two unstaggered DSWs with large velocity ($\lambda=+2.5$). (b) On-site collision of the same DSWs but without velocity formation of a quasibound state. (c) Collision of the same DSWs as in (b) but collision site between two waveguides—formation of a moving DSW. (d) Collision of two DSWs of different topology ($\lambda=\pm 2.5$)—“annihilation” of DSWs; contour lines at 0.5, 1, 2.

If two DSWs of different topology (staggered and unstaggered) collide their interaction results in a complete destruction of both DSWs and the emission of a dispersive wave [see Fig. 6(d)]. Hence in some respect staggered DSWs can be regarded as “antiparticles” of staggered DSW because the collision of both DSWs evokes their mutual annihilation.

V. CONCLUSIONS

In conclusion we have shown that in contrast to the cubic case bright solitary waves of different topology (staggered and unstaggered) can exist in the same waveguide array with a quadratic nonlinearity. Even discrete solitary wave solutions always turned out to be unstable. Either the staggered or the unstaggered DSWs (which depends on the mismatch) exhibit a power threshold if the respective wave vector approaches the linear wave vector band determined by the SH. Beyond this threshold two kinds of odd and even solutions exist. The odd DSW the Hamiltonian of which is closer to that of linear waves decays into those linear waves. As in the cubic case the solitary waves can move across the array provided that their power is sufficiently small and that coupling between the FHs is taken into account. If the power and likewise the Peierls-Nabarro barrier grows larger the solutions get progressively stronger localized. The collision behavior critically depends on the velocity and topology of the solutions as well as the site of collision.

ACKNOWLEDGMENT

The authors acknowledge a grant from the Deutsche Forschungsgemeinschaft, Bonn, in the framework of the initiative on “Optical Signal Processing.”

[1] G. I. Stegeman, D. J. Hagan, and L. Torner, *Opt. Quantum Electron.* **28**, 1691 (1996).
 [2] G. Assanto, *Opt. Lett.* **20**, 1595 (1995).
 [3] W. E. Toruellas, Z. Wang, D. J. Hagan, E. W. VanStryland, G. I. Stegeman, L. Torner, and C. R. Menyuk, *Phys. Rev. Lett.* **74**, 5036 (1995).
 [4] A. Kobayakov and F. Lederer, *Phys. Rev. D* **54**, 3455 (1996).

[5] L. Torner, D. Mazilu, and D. Mihalache, *Phys. Rev. Lett.* **77**, 2455 (1996).
 [6] C. Etrich, U. Peschel, F. Lederer, and B. A. Malomed, *Phys. Rev. E* **55**, 6155 (1997).
 [7] T. Peschel, U. Peschel, F. Lederer, and B. A. Malomed, *Phys. Rev. E* **55**, 4730 (1997).
 [8] E. Fermi, J. Pasta, and S. Ulam (unpublished).

- [9] A. B. Aceves, C. De Angelis, T. Peschel, R. Muschall, F. Lederer, S. Trillo, and S. Wabnitz, *Phys. Rev. E* **53**, 1172 (1996).
- [10] W. Krolilowski and Y. S. Kivshar, *J. Opt. Soc. Am. B* **13**, 876 (1996).
- [11] Y. N. Karamzin and A. P. Sukhorukov, *Zh. Eksp. Teor. Fiz.* **68**, 834 (1975) [*Sov. Phys. JETP* **41**, 414 (1976)].
- [12] R. Schiek, *Opt. Quantum Electron.* **26**, 415 (1994).
- [13] R. Schiek, Y. Baek, and G. I. Stegeman, *Phys. Rev. E* **53**, 1138 (1995).
- [14] R. Schiek, Y. Baek, G. Krijnen, and G. I. Stegeman, *Opt. Lett.* **21**, 940 (1996).
- [15] D. Cai, A. R. Bishop, and N. Gronbech-Jensen, *Phys. Rev. Lett.* **72**, 591 (1994).
- [16] A. C. Scott and MacNeil, *Phys. Lett. A* **98**, 87 (1983).
- [17] A. V. Buryak and Y. S. Kivshar, *Phys. Lett. A* **197**, 407 (1995).
- [18] J. B. Page, *Phys. Rev. B* **41**, 7835 (1990).
- [19] Y. A. Kivshar and D. K. Campbell, *Phys. Rev. E* **53**, 1138 (1995).
- [20] C. Etrich, U. Peschel, F. Lederer, B. A. Malomed, and Y. S. Kivshar, *Phys. Rev. E* **54**, 4321 (1996).
- [21] C. Etrich, U. Peschel, F. Lederer, and B. A. Malomed, *Phys. Rev. A* **52**, R3444 (1995).